Transient lasing without inversion via forbidden and virtual transitions

Luqi Yuan,[1] Dawei Wang,[1] Anatoly A. Svidzinsky,[1] Hui Xia,[2] Olga Kocharovskaya,[1] Alexei Sokolov,[1] George R. Welch,[1] Szymon Suckewer,[2] and Marlan O. Scully[1,2,3]

[1]*Texas A&M University, College Station, Texas 77843, USA*

[2]*Princeton University, Princeton, New Jersey 08544, USA*

[3]*Baylor University, Waco, Texas 76706, USA*

(Received 2 March 2013; published 13 January 2014)

Lasing without inversion (LWI) in the extreme-ultraviolet (XUV) has been the focus of recent research of our Princeton/Texas group. Because of the restriction imposed on the decay rates associated with the usual LWI schemes, it is difficult to transfer the physics gleaned from previous experiments to the XUV. However, with the advent of tunable-ultrashort-high-power laser pulses, we find that the possibility of transient LWI holds promise for a different LWI paradigm in which the lasing is based on forbidden and/or virtual transitions. It is the purpose of the present paper to present simple but (hopefully) convincing arguments and suggest realistic experiments to stimulate interest in this idea.

DOI: 10.1103/PhysRevA.89.013814 PACS number(s): 42.50.Gy

I. INTRODUCTION

The effects of atomic coherence [1–18] in laser physics have been the subject of substantial theoretical and experimental study. For example, mitigation of spontaneous emission effects (in order to reduce the laser linewidth) in the correlated emission laser have been predicted [19,20] and observed [21]. These studies introduced coherence between two upper laser levels. Similar upper level coherences have been shown [22] to enhance, in principle, the efficiency of photocells by mitigating radiative emission. On the other hand, absorption reduction via quantum coherence has been demonstrated theoretically [1–3] and experimentally [23] to yield lasing without inversion (LWI).

Coherence between excited and lower-level doublets is frequently associate with Λ and V atomic configurations as in Fig. 1. In the past, LWI experiments typically required $\gamma_{a\to c}$ in Λ and $\gamma_{c\to b}$ in V systems to be greater than $\gamma_{a\to b}$. Here $\gamma_{i\to j}$ is the spontaneous decay rate from level i to level j. The physical reason for this condition on the rates can be seen by considering the dark and bright states in the Λ system as an example,

$$|D\rangle = \frac{\Omega_l|c\rangle - \Omega_d|b\rangle}{\sqrt{\Omega_l^2+\Omega_d^2}}, \tag{1}$$

$$|B\rangle = \frac{\Omega_d|c\rangle + \Omega_l|b\rangle}{\sqrt{\Omega_l^2+\Omega_d^2}}. \tag{2}$$

The drive field Rabi frequency Ω_d is much larger than the lasing field Rabi frequency Ω_l. Thus, if the injection is in the state $|c\rangle$, then there is a (small) probability $\Omega_l/\sqrt{\Omega_l^2+\Omega_d^2}$ of finding the atom in the dark state where it never absorbs laser radiation. There is a larger probability $\Omega_d/\sqrt{\Omega_l^2+\Omega_d^2}$ of injection in the bright state. The bright state can be excited to the $|a\rangle$ level where the atom can decay to $|c\rangle$ with a rate $\gamma_{a\to c}$, and the process is repeated. Every cycle has a chance of emitting a laser photon and going into the dark state. However, if the atom decays from state $|a\rangle$ to state $|b\rangle$ (with a rate $\gamma_{a\to b}$), then this atom is lost from the game (without contributions to the laser) since it is essentially the $|b\rangle$ state in the dark state $|D\rangle$ for $\Omega_d \gg \Omega_l$.

The decay rate on the drive transitions must be greater than the decay rate of the lasing transitions $\gamma_{a\to b}$. This is bad news for x-ray LWI, where the high-frequency $a \to b$ lasing transition generally decays faster than the lower-frequency drive transition [5]. However (and this is the basis of our present transient XUV-LWI [24–26] studies), for high-power subpicosecond pulses, decay rates are of secondary importance. In particular, the present paper has been stimulated by and is an extension of our recent experiment [27] of atomic coherence effects in the triplet manifold of helium and helium-like ions (see Fig. 2). In that experiment, we were able to observe superradiance in plasma, and we are thus encouraged to extend the scope of our work to include LWI atomic coherence effects solely in the triplet manifold. It is interesting to note, however, that the present studies also involve lasing on "forbidden" and "virtual" transitions. In particular, we present here an analysis of the laser physics of a driven V system in a dressed state basis demonstrating XUV short pulse amplification without population inversion. The strong drive laser is treated to all orders in the drive Rabi frequency Ω_d while the weak laser is treated to lowest order in Ω_l, as indicated in Fig. 3. The possibility of transient XUV-LWI is an alternative of the current XUV technologies [28–35]. The next section sketches the V LWI analysis of the laser pulse amplification of a weak ultrashort laser seed pulse in the presence of a strong driving pulse. The case of near resonance ($\Delta \approx 0$) is given in Sec. III and the case of large detuning ($\Delta \gg \Omega_d$) is given in Sec. IV. Numerical simulations on helium atoms or helium-like ions for proposed experimental realization are in Sec. V. We present our conclusion in Sec. VI.

II. SHORT PULSE AMPLIFICATION WITHOUT INVERSION

To present the physics of transient LWI in the simplest terms, we consider an ensemble of independent stationary atoms lasing on the $a \to b$ and driven on the $c \to b$ legs of

 ©2014 American Physical Society

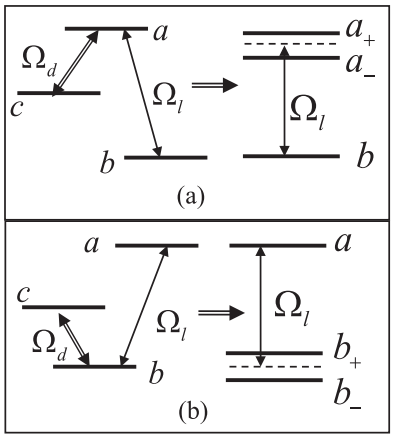

FIG. 1. Upper (a) [lower (b)] level doublet in the dressed state basis as produced by a drive laser between a and c (b and c). The drive Rabi frequency is Ω_d and the laser Rabi frequency is Ω_l. The double line means a much larger Rabi frequency in the drive transition than the Rabi frequency in the lasing transition, as indicated by the single line.

a V configuration. A dressed state picture of such a setup is depicted in Fig. 4.

In the usual slowly varying approximation, the laser Rabi frequency (between a and b) changes slowly on the state of $1/\nu_l$, where ν_l is the laser frequency and it is governed by the equation of motion

$$\left(\frac{\partial}{\partial z}+\frac{1}{c}\frac{\partial}{\partial t}\right)\Omega_l(z,t)=i\eta(\rho_{a+}e^{-i\omega_+ t}+\rho_{a-}e^{-i\omega_- t})e^{i\nu_l t-ik_l z}, \tag{3}$$

where for typographical convenience we denote ρ_{ab_+} by ρ_{a+}, etc., and $\eta=\frac{3}{8\pi}N\lambda_l^2\gamma$ in which γ is the radiative decay rate, $\lambda_l=c/\nu_l$ is the wavelength, and N is the atomic density. The density matrix elements $\rho_{a\pm}$ obey the Schrödinger equation

$$\begin{aligned}\dot{\rho}_{a+}=&-\Gamma\rho_{a+}-i\big[\Omega_{a+}\rho_{++}e^{-i(\nu_l-\omega_+)t}\\&+\Omega_{a-}\rho_{-+}e^{-i(\nu_l-\omega_-)t}-\Omega_{a+}\rho_{aa}e^{-i(\nu_l-\omega_+)t}\big],\end{aligned} \tag{4}$$

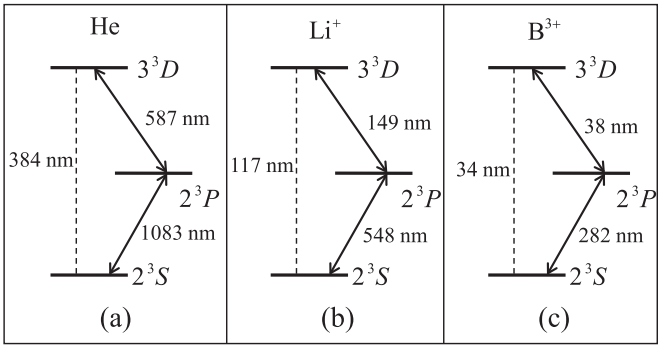

FIG. 2. Ladder level diagram of helium (a), helium-like Li^+ (b), and helium-like B^{3+} corresponding to the recent experiments [27] showing coherence between 2 ^3S and 2 ^3P in a helium-like plasma. The dashed line corresponds to the forbidden transition between 2 ^3S and 3 ^3D and the solid line corresponds to the allowed transitions.

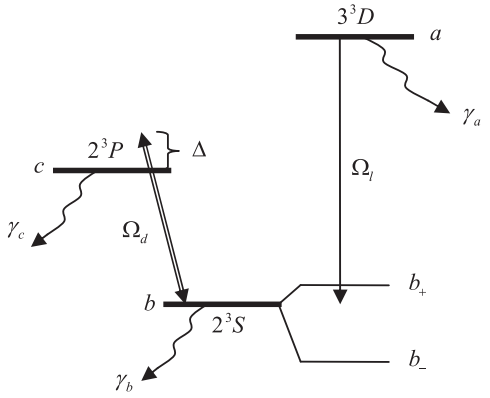

FIG. 3. V scheme with drive frequency $\nu_d=\omega_{cb}+\Delta$ and laser action $a\to b_\pm$. Decay of levels a, b, c at rates γ_a, γ_b, γ_c is to other levels outside the V system. The $\pm$ dressed states are indicated as subscripts on the atomic states, as discussed further in Appendix.

where the decay rate Γ is given by

$$\Gamma=\frac{\gamma_a+\gamma_c}{2}+\gamma_{\text{collision}}, \tag{5}$$

where we take the decay rates $\gamma_c=\gamma_b$ from the present purpose of resonant drive, and the Rabi frequencies $\Omega_{a\pm}$ are defined by

$$\Omega_{a\pm}=\frac{E}{\hbar}\langle a|e\vec{r}|b_\pm\rangle=\frac{E}{\hbar}\langle a|e\vec{r}\frac{1}{\sqrt{2}}[|b\rangle\pm|c\rangle]. \tag{6}$$

Then the eigenstates $|\Psi^\pm_{b,n}\rangle$ are [see Eq. (A11) in Appendix]

$$|\Psi^\pm_{b,n}\rangle=\frac{1}{\sqrt{2}}|b,n\rangle\pm\frac{1}{\sqrt{2}}|c,n-1\rangle. \tag{7}$$

III. RESONANT ($\Delta=0$) UNIFORM DECAY ($\gamma_b=\gamma_c$) CASE

The limit of resonant drive $\nu_d=\omega_{cb}$ and equal decay rates from c and b (due perhaps to atom or electron collisions) is instructive. Now the laser frequency lies midway between b_+

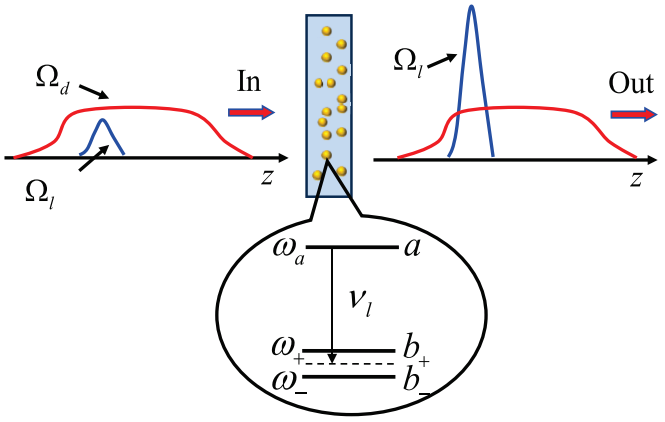

FIG. 4. (Color online) Incident laser pulse (Rabi frequency Ω_l) and drive pulse (Rabi frequency Ω_d) pass through gas or plasma in which the lasing atoms are in a coherent superposition of a dressed state $|b_\pm\rangle$. The dashed line between b_+ and b_- indicates the position of level b when $\Omega_d=0$.

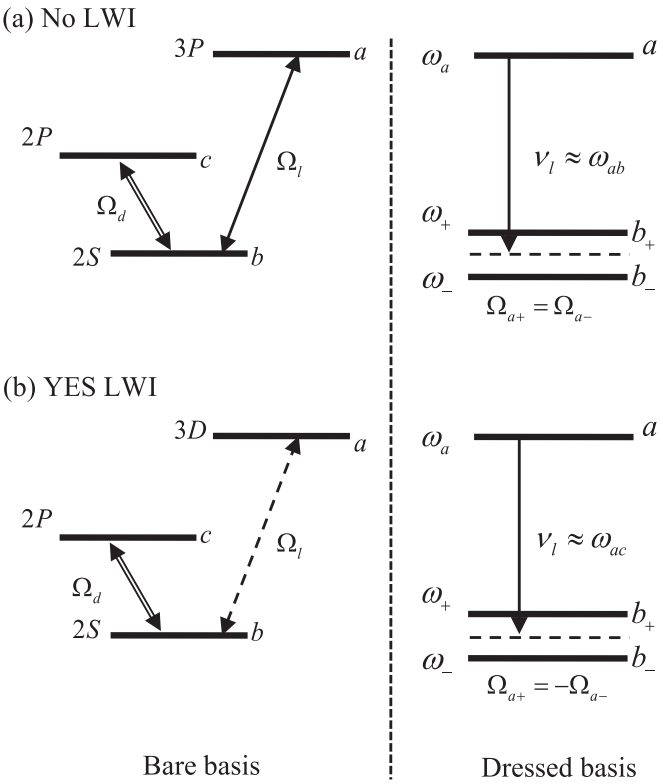

FIG. 5. (a) The usual V scheme, which does not yield LWI; (b) the "V" scheme in which the $|a\rangle \to |b\rangle$ transition is forbidden (dashed double-arrow line) does yield LWI at the frequency $\nu_l \approx \omega_{ac}$.

and b_-, that is, $\nu_l = \frac{1}{2}(\omega_+ + \omega_-)$, where $\omega_+ - \omega_- = \Omega_d$. In the short pulse limit such that $\tau_{\rm pulse}^{-1} \gg \Omega \gg \Gamma$, after time τ, Eq. (4) yields

$$\rho_{a+}(\tau) \approx i\tau\,\{\Omega_{a+}[\rho_{++}(0) - \rho_{aa}(0)] + \Omega_{a-}\rho_{-+}(0)\}\,. \quad (8)$$

At time $t = 0$, we populate the upper and lower laser levels such that $\rho_{aa} + \rho_{bb} = 1$. The drive level c is not populated so that $\rho_{cc} = 0$. In such a case, the dressed states are now

$$|b\pm\rangle = \frac{1}{\sqrt{2}}[|b\rangle \pm |c\rangle]. \quad (9)$$

The lower laser state in the $|\pm\rangle$ representation is

$$|b\rangle = \frac{1}{\sqrt{2}}[|b_+\rangle + |b_-\rangle]. \quad (10)$$

Hence for the initial density matrix

$$\begin{aligned}\rho(0) &= \rho_{aa}(0)|a\rangle\langle a| + \rho_{bb}(0)|b\rangle\langle b| \\ &= \rho_{aa}(0)|a\rangle\langle a| + \tfrac{1}{2}\rho_{bb}(0) \\ &\quad\times [|b_+\rangle\langle b_+| + |b_-\rangle\langle b_-| + |b_+\rangle\langle b_-| + |b_-\rangle\langle b_+|]\,,\end{aligned} \quad (11)$$

so that

$$\rho_{++}(0) = \rho_{--}(0) = \tfrac{1}{2}\rho_{bb}(0) \quad (12)$$

and

$$\rho_{+-}(0) = \rho_{-+}(0) = \tfrac{1}{2}\rho_{bb}(0). \quad (13)$$

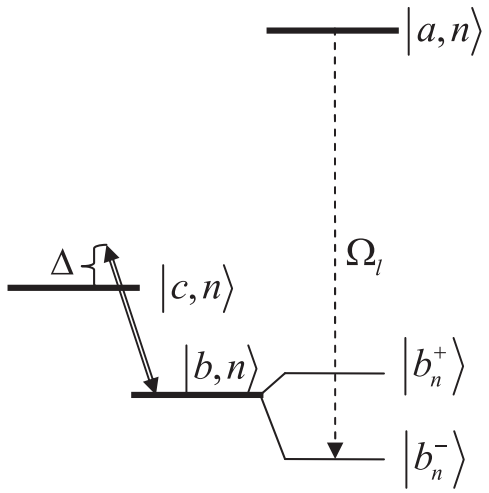

FIG. 6. Dressed state $|b_n^\pm\rangle$ with their frequencies $\omega_b^+ \approx \omega_b + n\nu_d - i\frac{\gamma_b}{2} + \frac{\Omega_n^2}{4\Delta}$ and $\omega_b^- \approx \omega_b + n\nu_d - i\frac{\gamma_c}{2} - \Delta + \frac{\Omega_n^2}{4\Delta}$ for the case $\Delta \gg \Omega_n$. $|b_n^+\rangle = \sqrt{1 - \frac{|\Omega_n^2|}{4\tilde{\Delta}^2}}|b,n\rangle + \sqrt{\frac{|\Omega_n^2|}{4\tilde{\Delta}^2}}|c,n-1\rangle$ and $|b_n^-\rangle = \sqrt{\frac{|\Omega_n^2|}{4\tilde{\Delta}^2}}|b,n\rangle - \sqrt{1 - \frac{|\Omega_n^2|}{4\tilde{\Delta}^2}}|c,n-1\rangle$. $\tilde{\Delta} = \Delta + \frac{i}{2}(\gamma_c - \gamma_b)$ and $\nu_l \approx \omega_{ab} - \nu_d - \Omega^2/4\Delta$. (See Appendix for details.)

We consider the Rabi frequencies $\Omega_{a\pm}$ as defined in Eq. (6) and then proceed to calculate ρ_{a+}. Thus we see that if, for example, $|a\rangle = |3P\rangle$, $|b\rangle = |2S\rangle$, then Eq. (6) gives $\Omega_{a+} = \Omega_{a-}$. Equation (8) yields $\rho_{a+}(\tau) = i\tau\,\{\Omega_{a+}[\rho_{bb}(0) - \rho_{aa}(0)]\}$. This implies that $\mathrm{Im}[\rho_{a+}(\tau)] > 0$ for no population inversion, so LWI is not realized. However, if $|a\rangle = |3D\rangle$ and $|b\rangle = |2S\rangle$, then $\Omega_{a+} = -\Omega_{a-}$. In this case, Eq. (8) yields $\rho_{a+}(\tau) = -i\tau\,\{\Omega_{a+}\rho_{aa}(0)\}$, which implies that $\mathrm{Im}[\rho_{a+}(\tau)] < 0$. Therefore, combining the equation of motion for the field [Eq. (3)], we have the LWI gain given by

$$\text{gain} \approx \frac{3}{8\pi}N\lambda^2\gamma\tau\rho_{aa}^{(0)}. \quad (14)$$

This is summarized in Fig. 5. Although the solution in this section is insightful, we should emphasize that the "V" scheme in Fig. 5(b) is actually a ladder scheme. The "LWI" at the "forbidden" transition has a lasing frequency close to ω_{ac}.

IV. LARGE DETUNING BETWEEN b_+ AND b_- STATES

For large Ω_d with negligible γ and Δ, the $\omega_\pm$ frequencies are governed by Ω_d. In this case, it is useful to offset the laser frequency ν_l by $\pm\Omega_d$, i.e., to generate side bands so that $E_0(z,t)e^{i\nu t} \to E'(z,t)[e^{i(\nu+\Omega_d)t} + e^{i(\nu-\Omega_d)t}]$. The Hamiltonian is then

$$\begin{aligned}V(t) &= \wp_{ac}[|a\rangle\langle b_+|e^{i\omega_+ t} + |a\rangle\langle b_-|e^{i\omega_- t}]E \\ &\quad\times [e^{-i(\nu+\Omega_d)t} + e^{-i(\nu-\Omega_d)t}] + \text{adj.} \\ &= \wp_{ac}E[|a\rangle\langle b_+|(1 + e^{i(\omega_+ - \nu+\Omega_d)t}) \\ &\quad + |a\rangle\langle b_-|(1 + e^{i(\omega_- - \nu-\Omega_d)t})] + \text{adj.}\end{aligned} \quad (15)$$

since $\omega_\pm = \nu \pm \Omega_d$, and ignoring the rapidly oscillating terms in Eq. (15), we have the LWI gain as the same as that in Eq. (14).

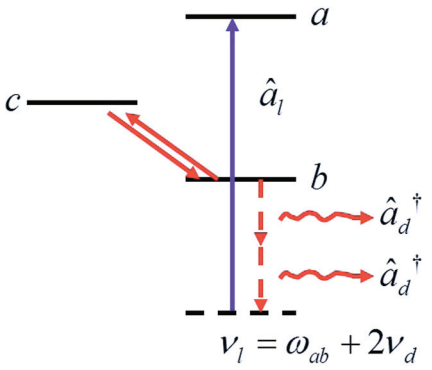

FIG. 7. (Color online) The schematic energy level scheme for the high-order gain.

The limit of large detuning, $\Delta \gg \Omega_d \gg \gamma_a, \gamma_b$, is of interest, as sketched in Fig. 6. To realize laser amplification with more atoms in the b state than in the a state and when state c is initially empty, we note that the density matrix is then

$$\rho(0) = \rho_{aa}|a\rangle\langle a| + \rho_{bb}|b\rangle\langle b|. \tag{16}$$

We may write the $|b\rangle$ state in the $|\pm\rangle$ basis in the large Δ limit of Fig. 6 as

$$|b\rangle = \sqrt{1 - \frac{\Omega^2}{4\tilde{\Delta}^2}}|b_+\rangle - \sqrt{\frac{\Omega^2}{4\tilde{\Delta}^2}}|b_-\rangle, \tag{17}$$

where $\tilde{\Delta} \equiv \Delta + \frac{i}{2}(\gamma_c - \gamma_b)$. Hence most of the lower-level population is in b_+ since $\Delta \gg \Omega$, and $\rho_{--} \approx \frac{\Omega^2}{4\Delta^2}\rho_{bb}$. In such a case, we have the chance to get population inversion between level $|a\rangle$ and level $|b_-\rangle$, and lasing action is indicated to take place between $|a,n\rangle$ and $|b,n\rangle$. The lasing frequency is then $\nu_l \approx \omega_{ab} + \Delta$.

Higher laser frequencies can be obtained, and this gain is understood as involving virtual transitions as indicated in Fig. 7. The atom at level b emits a photon with frequency ν_d but gets excited to level c via the virtual process. It then emits another photon and decays to the ground state b. Hence the atom is back to the ground state but its energy is shifted by $2\nu_d$. Higher laser frequency can also be achieved in the ladder scheme for the same reason. In principle, such a mechanism can generate higher-order sidebands in LWI. We will discuss this possibility elsewhere [36]. In the next section, we will provide a numerical study to prove these mechanisms with realistic numbers.

V. EXPERIMENTAL PROPOSAL

We choose the triplet levels of helium atoms or helium-like ions for proposed experimental realization of the above concept. Our approach utilizes advantages of the recombination XUV lasers [28,29] and the effects of quantum coherence. The population in the excited state atoms is prepared through optical field ionization followed by nonradiative three-body (two electrons and one ion) recombination, as described in [27]. For three-body recombination rates to dominate collisional ionization rates, the recombining plasma should have a low electron temperature. Low-temperature plasma can be realized with ultrashort laser pulses (at intensity on the order of 10^{15} W/cm^2 for helium) through tunneling ionization [37–39]. Use of ultrashort laser pulses is crucial to minimize plasma heating. A Ti:sapphire laser at wavelength 800 nm with pulses of 30–100 fs duration can be used to generate the plasma. It has been demonstrated that a 4-mm-long plasma channel can be achieved with the aid of Axicon lenses [40].

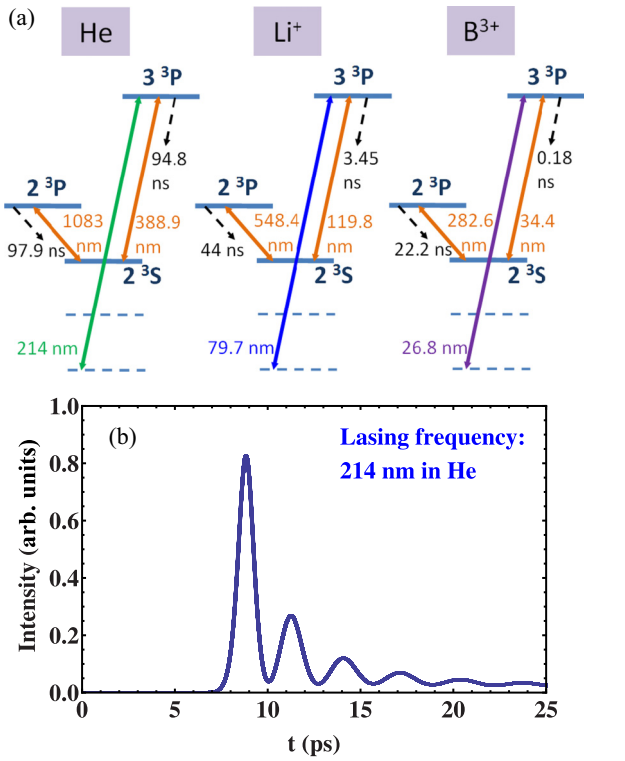

FIG. 8. (Color online) (a) Energy diagrams (S-P-P scheme) of He, Li^+, and B^{3+}; (b) simulated output intensity of the lasing fields vs time.

We first give three experimental proposals in an S-P-P scheme with helium [Fig. 8(a)]. This is a V-like scheme. The drive laser is provided by an Nd:YAG laser or its second or fourth harmonic, and is used to drive the $2\,^3S \leftrightarrow 2\,^3P$ transition of the helium atoms. The lasing transition in which we are interested is from the $3\,^3P$ to the virtual level at the wavelength of the UV regime. We choose the typical experimental parameters and conditions as follows. The atomic system has density 10^{18} cm^{-3} and we prepare 15% population at the exited state $3\ ^3P$. The system has a decoherence rate of 0.3×10^{11} s^{-1} and a length of 1 mm. We pump the lower transition with a strong laser pulse at 1064 nm wavelength, with 1 mJ energy/pulse and ~30 ps pulse duration. We send the seed which is near resonant with the $3\ ^3P \rightarrow 2\,^3S$ transition and has energy ~10 pJ. Lasing without inversion at the resonant frequency is emitted in the transient regime. Furthermore, we also detect the emission at the higher frequency (~214 nm) and find the emission energy at this frequency is ~1 nJ. The time evolution of the intensity of the lasing emission at 214 nm wavelength versus time is presented in Fig. 8(b).

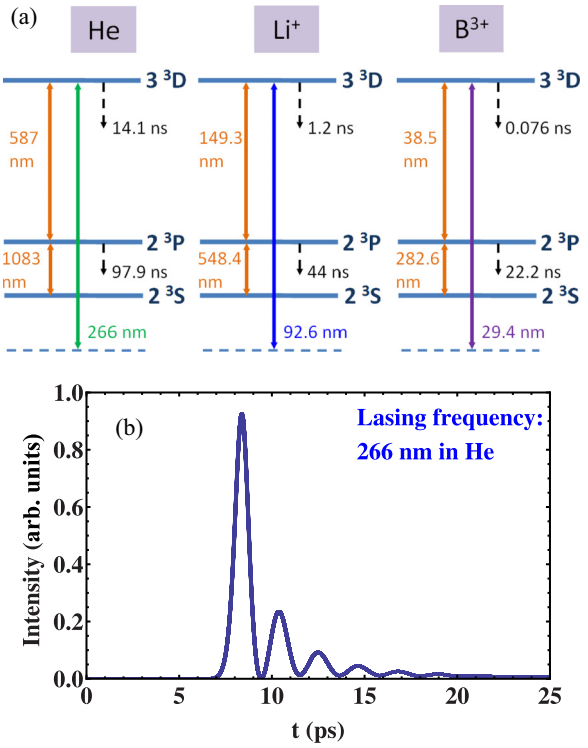

FIG. 9. (Color online) (a) Energy diagrams (S-P-D scheme) of He, Li^+, and B^{3+}; (b) simulated output intensity of the lasing fields vs time.

We also show the gain in the S-P-D scheme with helium. This time, we choose the same drive field as we used in the previous calculation, but we only need the atom medium with 10^{17} cm^{-3} and 10% population prepared at the exited state 3 ^3D. The seed pulse has the same energy, ∼10 pJ, but a wavelength of ∼587 nm. The output lasing without inversion also has the frequency component at ∼266 nm and corresponding energy ∼1 nJ. [We show similar temporal behavior of the output field at the wavelength ∼266 nm in Fig. 9(b).] These calculations can be extended to other helium-like ions such as Li^+ and B^{3+} with energy schemes shown in Figs. 8(a) and 9(a).

Although the experimental conditions for both proposals are different, there is no fundamental difference between the mechanism of generation of higher-frequency lasing without population inversion in the S-P-P and the S-P-D schemes. In a sample as short as 1 mm, we achieve a nano-Joule emission via the virtual process. Experiments may be complicated by requirements of high atomic density, etc. Nevertheless, the high-frequency field amplification without population inversion driven by a low-frequency intensive field holds real promise.

VI. CONCLUSION

Previous proposals of LWI are constrained by special requirements on spontaneous decay rates of atomic transitions which limit their practical implementation. Here we show that LWI can be achieved on a fast superradiant time scale in a transient regime which lifts unwanted limitations and yields potential for generation of coherent XUV or x-ray by driving an atomic system with a low-frequency (e.g., infrared) field. In our approach, LWI occurs on a "forbidden" transition and also can result in light amplification at a higher frequency due to the virtual process. We sketch the V scheme LWI analysis in a dressed state basis where a weak ultrashort laser seed pulse is amplified by using a strong driving field. Experimental proposals of the concept in three-level helium atoms or helium-like ions are investigated numerically. We find that the higher-frequency laser field can be generated in both S-P-P and S-P-D schemes. The analysis in this paper is simple but the results are exciting. We hope this will stimulate further discussions and more ideas in this area.

ACKNOWLEDGMENTS

The authors acknowledge the support of the National Science Foundation Grants No. PHY-1241032 (INSPIRE CREATIV) and No. PHY-1205868 and the Robert A. Welch Foundation (Awards A-1261 and A-1547). L.Y. is supported by the Herman F. Heep and Minnie Belle Heep Texas A&M University Endowed Fund held/administered by the Texas A&M Foundation.

APPENDIX: BARE ESSENTIALS OF DRESSED STATES

For the convenience of the reader and to establish the notation, we present here the analysis of the driven levels c and b which are decaying to other far-detuned states. This is a well-studied problem, but it is central to our calculation and we do not find that the usual treatment contains all the details we want, e.g., eigenvectors including decay, detuning, etc. To that end, we consider an n photon drive field of frequency ν_d interacting with the b, c two-level system. As in Fig. 3, the state vector is given by

$$|\Psi\rangle = c_n(t)|c,n\rangle + b_{n+1}(t)|b,n+1\rangle, \tag{A1}$$

and the probability amplitudes obey the equation of motion

$$\dot{c}_n = \left[-i(\omega_c + n\nu) - \frac{\gamma_c}{2}\right]c_n - ig\sqrt{n+1}b_{n+1}, \tag{A2}$$

$$\dot{b}_{n+1} = \left[-i[\omega_b + (n+1)\nu] - \frac{\gamma_b}{2}\right]b_{n+1} - ig^*\sqrt{n+1}c_n, \tag{A3}$$

where g is the complex atom-field coupling frequency. As indicated in Fig. 3, $\nu = \omega_{cb} + \Delta$, where $\omega_{cb} = \omega_c - \omega_b$ and Δ is the detuning between the drive field frequency and the $c \to b$ transition frequency. We may write the matrix analog of Eqs. (A2) and (A3) as

$$\frac{d}{dt}\begin{pmatrix} c_n \\ b_{n+1} \end{pmatrix} = -i\begin{bmatrix} \omega_c + n\nu - i\gamma_c/2 & g\sqrt{n+1} \\ g^*\sqrt{n+1} & \omega_c + n\nu + \Delta - i\gamma_b/2 \end{bmatrix} \times \begin{pmatrix} c_n \\ b_{n+1} \end{pmatrix}, \tag{A4}$$

where we have used the fact that $\omega_b + \nu = \omega_c + \Delta$. It is convenient to write Eq. (A4) as

$$\frac{d}{dt}\begin{pmatrix} c_n \\ b_{n+1} \end{pmatrix} = -i\left\{(\omega_c + n\nu + \Delta/2)\begin{bmatrix} 1 & 0 \\ 0 & 1 \end{bmatrix} + \frac{1}{2}\begin{bmatrix} -\Delta - i\gamma_c & \Omega_n \\ \Omega_n^* & \Delta - i\gamma_b \end{bmatrix}\right\}\begin{pmatrix} c_n \\ b_{n+1} \end{pmatrix}, \quad \text{(A5)}$$

where $g\sqrt{n+1} = \frac{1}{2}\Omega_n$. The eigenfrequency of the $|c,n\rangle$, $|b,n+1\rangle$ pair is then

$$\lambda_{c,n}^{(\pm)} = \omega_c + n\nu + \frac{\Delta}{2} - i\frac{\gamma_c + \gamma_b}{4} + R_n^{(\pm)}, \quad \text{(A6)}$$

where the generalized Rabi frequency is

$$R_n^{(\pm)} = \pm\frac{1}{2}\left[\left(\Delta + \frac{i}{2}(\gamma_c - \gamma_b)\right)^2 + |\Omega_n|^2\right]^{1/2}. \quad \text{(A7)}$$

The lower level b with n photons, $|b,n\rangle$, coupled to the state $|c,n-1\rangle$ replacing $n \to n-1$ and using $\nu = \omega_{cb} + \Delta$ in Eq. (A4) yields

$$\begin{aligned}\frac{d}{dt}\begin{pmatrix} c_{n-1} \\ b_n \end{pmatrix} &= -i\begin{bmatrix} \omega_b + n\nu - \Delta - i\gamma_c/2 & g\sqrt{n} \\ g^*\sqrt{n} & \omega_c + n\nu - i\gamma_b/2 \end{bmatrix}\begin{pmatrix} c_{n-1} \\ b_n \end{pmatrix} \\ &= -i\left\{(\omega_c + n\nu - \Delta/2)\begin{bmatrix} 1 & 0 \\ 0 & 1 \end{bmatrix}\right. \\ &\quad \left. + \frac{1}{2}\begin{bmatrix} -\Delta - i\gamma_c & \Omega_{n-1} \\ \Omega_{n-1}^* & \Delta - i\gamma_b \end{bmatrix}\right\}\begin{pmatrix} c_{n-1} \\ b_n \end{pmatrix}, \quad \text{(A8)}\end{aligned}$$

the eigenfrequency of the $|c,n-1\rangle$, $|b,n\rangle$ pair is

$$\lambda_{b,n}^{(\pm)} = \omega_b + n\nu - \frac{\Delta}{2} - i\frac{\gamma_c + \gamma_b}{4} + R_{n-1}^{(\pm)}, \quad \text{(A9)}$$

and the eigenvectors are found to be

$$|\Psi_{c,n}^{\pm}\rangle = \frac{1}{2}\sqrt{\frac{|\Omega_n|^2}{R_n^{(\pm)}\left[2R_n^{(\pm)} + \Delta + \frac{i}{2}(\gamma_c - \gamma_b)\right]}}|c,n\rangle \pm \frac{1}{2}\sqrt{\frac{2R_n^{(\pm)} + \Delta + \frac{i}{2}(\gamma_c - \gamma_b)}{R_n^{(\pm)}}}|b,n+1\rangle, \quad \text{(A10)}$$

$$|\Psi_{b,n}^{\pm}\rangle = \frac{1}{2}\sqrt{\frac{2R_{n-1}^{(\pm)} + \Delta + \frac{i}{2}(\gamma_c - \gamma_b)}{R_{n-1}^{(\pm)}}}|b,n\rangle \pm \frac{1}{2}\sqrt{\frac{|\Omega_{n-1}|^2}{R_{n-1}^{(\pm)}\left[2R_{n-1}^{(\pm)} + \Delta + \frac{i}{2}(\gamma_c - \gamma_b)\right]}}|c,n-1\rangle. \quad \text{(A11)}$$

[1] O. A. Kocharovskaya and Ya. I. Khanin, J. Exp. Theor. Phys. **48**, 630 (1988).
[2] S. E. Harris, Phys. Rev. Lett. **62**, 1033 (1989).
[3] M. O. Scully, S.-Y. Zhu, and A. Gavrielides, Phys. Rev. Lett. **62**, 2813 (1989).
[4] A. Imamoglu and S. E. Harris, Opt. Lett. **14**, 1344 (1989).
[5] A. Imamoglu, J. E. Field, and S. E. Harris, Phys. Rev. Lett. **66**, 1154 (1991).
[6] Y. Zhu, Phys. Rev. A **45**, R6149 (1992).
[7] M. Fleischhauer, A. Imamoglu, and J. P. Marangos, Rev. Mod. Phys. **77**, 633 (2005).
[8] X. J. Fan, N. Cui, H. Ma, A. Y. Li, and H. Li, Eur. Phys. J. D **37**, 129 (2006).
[9] H. Wu, M. Xiao, and J. Gea-Banacloche, Phys. Rev. A **78**, 041802 (2008).
[10] M. F. Pereira Jr., Phys. Rev. B **78**, 245305 (2008).
[11] V. Ahufinger, R. Shuker, and R. Corbalán, Appl. Phys. B **80**, 67 (2005).
[12] D. Braunstein and R. Shuker, J. Phys. B **42**, 125401 (2009).
[13] Y.-P. Sun, J.-C. Liu, C.-K. Wang, and F. Gel'mukhanov, Phys. Rev. A **81**, 013812 (2010).
[14] M. Marthaler, Y. Utsumi, D. S. Golubev, A. Shnirman, and G. Schön, Phys. Rev. Lett. **107**, 093901 (2011).
[15] D. Braunstein, G. A. Koganov, and R. Shuker, J. Phys. B **44**, 235402 (2011).
[16] G. A. Koganov, B. Shif, and R. Shuker, Opt. Lett. **36**, 2779 (2011).
[17] A. A. Svidzinsky, L. Yuan, and M. O. Scully, Phys. Rev. X **3**, 041001 (2013).
[18] R. W. Boyd, *Nonlinera Optics* (Academic, San Diego, 2003).
[19] M. O. Scully and M. S. Zubairy, Phys. Rev. A **35**, 752 (1987).
[20] M. O. Scully, Phys. Rev. Lett. **55**, 2802 (1985).
[21] M. Ohtsu and K. Y. Liou, Appl. Phys. Lett. **52**, 10 (1988).
[22] M. O. Scully, Phys. Rev. Lett. **104**, 207701 (2010).
[23] A. S. Zibrov, M. D. Lukin, D. E. Nikonov, L. Hollberg, M. O. Scully, V. L. Velichansky, and H. G. Robinson, Phys. Rev. Lett. **75**, 1499 (1995).
[24] S. Y. Kilin, K. T. Kapale, and M. O. Scully, Phys. Rev. Lett. **100**, 173601 (2008).
[25] A. A. Svidzinsky, L. Yuan, and M. O. Scully, New J. Phys. **15**, 053044 (2013).
[26] Y. V. Rostovtsev and M. O. Scully, J. Mod. Opt. **54**, 2607 (2007).
[27] H. Xia, A. A. Svidzinsky, L. Yuan, C. Lu, S. Suckewer, and M. O. Scully, Phys. Rev. Lett. **109**, 093604 (2012).
[28] J. Zhang, M. H. Key, P. A. Norreys, G. J. Tallents, A. Behjat, C. Danson, A. Demir, L. Dwivedi, M. Holden, P. B. Holden, C. L. S. Lewis, A. G. MacPhee, D. Neely, G. J. Pert, S. A. Ramsden, S. J. Rose, Y. F. Shao, O. Thomas, F. Walsh, and Y. L. You, Phys. Rev. Lett. **74**, 1335 (1995).

[29] S. Suckewer and P. Jaeglé, Laser Phys. Lett. **6**, 411 (2009).
[30] R. Keenan, J. Dunn, P. K. Patel, D. F. Price, R. F. Smith, and V. N. Shlyaptsev, Phys. Rev. Lett. **94**, 103901 (2005).
[31] H. T. Kim, I. W. Choi, N. Hafz, J. H. Sung, T. J. Yu, K.-H. Hong, T. M. Jeong, Y.-C. Noh, D.-K. Ko, K. A. Janulewicz, J. Tümmler, P. V. Nickles, W. Sandner, and J. Lee, Phys. Rev. A **77**, 023807 (2008).
[32] Y. Wang, E. Granados, M. A. Larotonda, M. Berrill, B. M. Luther, D. Patel, C. S. Menoni, and J. J. Rocca, Phys. Rev. Lett. **97**, 123901 (2006).
[33] Y. Wang, E. Granados, F. Pedaci, D. Alessi, B. Luther, M. Berrill, and J. J. Rocca, Nat. Photon **2**, 94 (2008).
[34] H. Kapteyn, O. Cohen, I. Christov, and M. Murnane, Science **317**, 775 (2007).
[35] T. Popmintchev, M.-C. Chen, D. Popmintchev, P. Arpin, S. Brown, S. Ališauskas, G. Andriukaitis, T. Balčiunas, O. D. Mücke, A. Pugzlys, A. Baltuška, B. Shim, S. E. Schrauth, A. Gaeta, C. Hernández-García, L. Plaja, A. Becker, A. Jaron-Becker, M. M. Murnane, and H. C. Kapteyn, Science **336**, 1287 (2012).
[36] L. Yuan, D.-W. Wang, A. A. Svidzinsky, and M. O. Scully, arXiv:1312.7855.
[37] X. M. Tong, Z. X. Zhao, and C. D. Lin, Phys. Rev. A **66**, 033402 (2002).
[38] V. S. Popov, Phys. Usp. **47**, 855 (2004).
[39] L. V. Keldysh, Sov. Phys. JETP **20**, 1307 (1965).
[40] D. Turnbull, S. Li, A. Morozov, and S. Suckewer, Phys. Plasmas **19**, 083109 (2012).